2013 IEEE/RSJ International Conference on
Intelligent Robots and Systems (IROS)
November 3-7, 2013. Tokyo, Japan

Discrete-Time Stability Analysis of a Control Architecture for Heterogeneous Robotic Systems

Magnus Bjerkeng, Pietro Falco, Ciro Natale and Kristin Y. Pettersen

Abstract— **The aim of this paper is to investigate the discrete-time stability of robot motion control in the task space. The control system has been modeled as a classical inner-loop/outer-loop architecture, adopted in several industrial robotic systems. The inner-loop is composed of a servo-level joint controller, and higher level kinematic feedback is performed in the outer-loop. Heterogeneous dynamics is considered in the inner-loop, which can for instance describe redundant coordination/synchronization control systems with cooperative robots with non-identical dynamical responses. There are surprisingly few discrete-time stability results in the current state-of-the-art for this popular control architecture. The qualitative effects of the inner-loop dynamics on the overall stability of the system is investigated, and improved outer-loop feedback gain margins are derived.**

I. INTRODUCTION

Historically, industrial manipulators have been adopted in highly structured environment, in which preprogrammed motion is sufficient to fulfill the assigned task and the perception of the external world is minimal. However, in modern, more flexible industrial scenarios the autonomy required for robotics systems is increasing and higher-level sensor based control techniques are needed in addition to pure motion control. A typical control hierarchy adopted in robotics and marine crafts is shown in Fig. 1, [1]. It is composed by two loops. The inner loop consists of low-level velocity controller of some configuration coordinates, i.e. the joint servo loop in robotics. The outer loop calculates the desired joint velocities using a kinematic controller usually taking extrasensory information into account.

Feedback for motion control of robotic systems in the control literature is usually considered in the continuous time framework, with torque as the control input [2]. However, most industrial robotic systems do not support direct torque control, offering instead a higher level discrete-time control interface [3]. Despite potentially lower performance, a hierarchical control design has advantages over centralized torque controllers with respect to modularity, portability, safety, and computational cost [4]. One of the most popular kinematic control laws used for outer-loop motion control is the *resolved motion rate controller* (RMRC) first proposed in [5]. This controller is the 1th order pseudoinverse *closed loop inverse kinematics* (CLIK) type controller proposed in [6] for closed loop motion control of robotic systems. Some applications of the RMRC include: Visual servoing [7], redundancy resolution (typically with respect to obstacle avoidance or manipulability) [8], multi-robot coordination [9], velocity-field control [10], or general operational-space trajectory tracking problems [11].

M. Bjerkeng and K. Y. Pettersen are with the Department of Engineering Cybernetics, Norwegian University of Science and Technology, NO-7491 Trondheim, Norway. {bjerkeng,Kristin.Y.Pettersen}@itk.ntnu.no

P. Falco and C. Natale are with the Dipartimento di Ingegneria dell'Informazione, Seconda Università degli Studi di Napoli, 81031 Aversa, Italy {pietro.falco,ciro.natale}@unina2.it

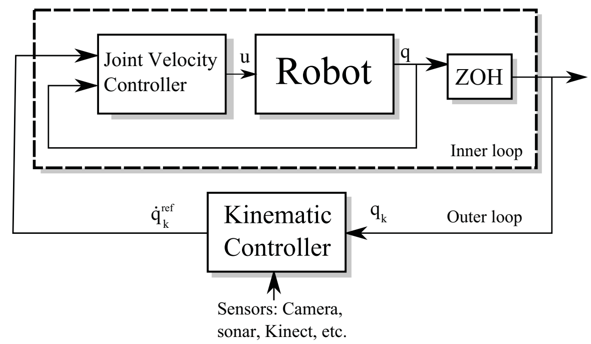

Fig. 1: Block diagram of a typical industrial robot motion control system. *Zero order hold* sampling of position measurements are available.

The practice of using outer loop RMRC to achieve operational space motions is well established (see, for example, [7]-[11]), the obtained stability properties, especially for discrete-time systems, have surprisingly not been the focus of much research.

Some notable results which have recently been presented for the continuous-time case include [4], where Lyapunov analysis is used to show uniform ultimate boundedness with a computed-torque type controller in the inner loop. Global exponential stability is reported in [12] using cascade theory, again with a computed-torque controller. Most recently uniform ultimate boundedness is shown using a PI-controller in the inner loop [13].

However, for discrete-time systems, hardly any results exist considering inner-loop dynamics. The assumption of no inner-loop dynamics reduces the system to the damped *Gauss-Newton method* for numerical optimization [14]. The latest result for this simplified system, [15] derives input bounds which are sufficient for local exponential stability of the equilibrium as well as a tight estimate of the region of attraction. The lack of general results in the literature for this popular motion control architecture is the main motivation behind this paper. The introduction of non-ideal effects resulting from heterogeneous inner-loop dynamics will give results which much better represent the realities faced when dealing with the control of industrial manipulators. The stability results presented hare are not only desirable for the completeness of literature, but also for determining how the inner-loop dynamics affects the overall stability of the closed loop system, especially with respect to outer loop feedback gains margins.

This paper represents a first step in understanding of the stability properties obtained using the RMRC in the discrete-time framework taking dynamics in the inner loop into account. The contributions in this paper are as follows.

- A heterogeneous dynamical model is introduced to accurately model systems consisting of cooperating agents with different dynamical responses, or robot manipulators where the response of the servo controllers for the different joints are non-identical.
- Experimental data from a real industrial manipulator is used to verify the proposed model.
- Stability results for the two-loop system are derived which is applicable to both minimum phase and non-minimum phase inner loop dynamics.
- Outer loop gain margins which ensure stability and simplify gain tuning are presented.

This paper is organized in the following way. The robot model is introduced in Section II. The stability problem statement is presented in Section III. The error dynamics are derived in Section IV followed by the Lyapunov-based stability proof in Section IV. Conclusions and further work is found in Section VII.

II. Robot model

In this section the low-level joint dynamical model and the notation used in this paper is introduced. It is stressed that the robot dynamics introduced now is the discrete input-output dynamics of the robot under servo control, i.e. the dashed box in Fig. 1. The reference velocity in the configuration space is the input, and the actual position is the output. We propose a linear model for these dynamics, which is for instance the case if feedback linearization or computed torque is used in the inner loop [4].

Consider a robotic system with configuration variables $\boldsymbol{q} \in \mathbb{R}^n$. The position at time $k \in \mathbb{Z}^+$ is given by $\boldsymbol{q}_k$ where the sampling period is T, where the continuous time is given by $t = Tk$. The low-level controller is passed a reference velocity $\dot{\boldsymbol{q}}_k^{\text{ref}}$ at time k. The measured joint increment $\Delta\boldsymbol{q}_k = \boldsymbol{q}_k - \boldsymbol{q}_{k-1}$ is assumed to converge exponentially to the reference for a constant reference velocity. Moreover, the low-level dynamics of each joint is assumed linearly decoupled. Denoting the convergence rate of Δq_i as $a_i \in (-1, 1)$ results in the following robot model

$$\Delta\boldsymbol{q}_{k+1} = \mathbf{A}\Delta\boldsymbol{q}_k + (\mathbf{I} - \mathbf{A})T\dot{\boldsymbol{q}}_k^{\text{ref}}, \tag{1}$$

where $\mathbf{A} = \text{diag}\{a_i\}$. A convergence rate of $a_i = 0$ corresponds to a perfect velocity controller which converges in one step, a_i close to 1 corresponds to a slow "overdamped" joint dynamics, and a_i close to -1 gives an oscillatory non-minimum phase response. The model is considered heterogeneous as the different states does not have an identical dynamical response. The homogenious case is when $a_i = a_j, \forall i, j$.

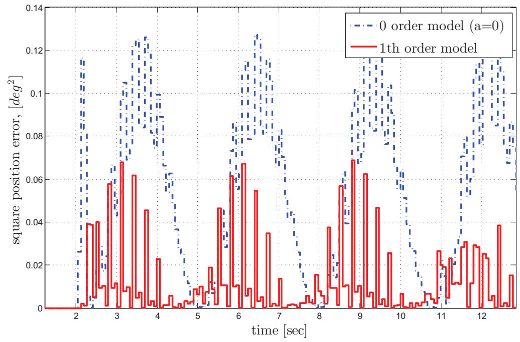

Fig. 2: 2-step ahead joint prediction errors using data from the KUKA-KR16 industrial manipulator with a sinusoidal reference. The mean square error of the 0th order model is about 5 times greater than the 1th order model.

Experimental data from a KUKA-KR16 manipulator was used to verify the model. The manipulator is composed of an elbow with 3 "large" servo motors, in series with a spherical wrist with 3 smaller servo motors. From input-output data of a KUKA-KR16 manipulator, a_{1-4} was identified around 0.6 with a sampling time of 75ms, and a_{5-6} had a faster convergence rate, around 0.5. Experimental data from a KUKA-KR16 as well as an identified 1th order input/output model of the servo-loop is seen if Fig. 2. It is seen that the prosed model more accurately describes the discrete joint dynamics than an algebraic model.

III. Problem statement

In this section the problem statement is presented, and we recall the RMRC for regulation.

Let $\boldsymbol{e} \in \mathcal{E}$ be the vector of task error variables of a robotic system, with $\mathcal{E}$ being a domain of $\mathbb{R}^m$, and let $\boldsymbol{q} \in \mathcal{Q}$ be the vector of the robotic system configuration, with $\mathcal{Q}$ being a domain of $\mathbb{R}^n$ with $m \leq n$, such that

$$\boldsymbol{e}(\boldsymbol{q}) : \mathcal{Q} \subseteq \mathbb{R}^n \mapsto \mathcal{E} \subseteq \mathbb{R}^m. \tag{2}$$

For example, in a robotic manipulator, $\boldsymbol{e}(\boldsymbol{q})$ may be the position error of the end effector, and $\boldsymbol{q}$ is the vector of joint positions, whereas in a platoon of mobile robots, $\boldsymbol{q}$ is the vector of coordinates representing the location of each robot, and $\boldsymbol{e}(\boldsymbol{q})$ is the vector of suitable task errors, depending on the mission. Note that for visual servoing $\boldsymbol{e}(\boldsymbol{q})$ depends upon camera information, but is still purely configuration dependent for a static scene. For distance-based formation control problems, [16], the task Jacobian may not be uniformly bounded. The results derived in this paper do not concern these control problems.

The robot is said to be executing its task if $\boldsymbol{e} = \mathbf{0}$. The task Jacobian is defined as $\mathbf{J}(\boldsymbol{q}) = \frac{\partial \boldsymbol{e}}{\partial \boldsymbol{q}} \in \mathbb{R}^{m \times n}$. For a *task redundant* problem we have $m < n$ using the definition in [17]. The problem is to determine if the RMRC given by Eq. (3) below can stabilize $\boldsymbol{e} = 0$ for the industrial robot dynamics (1). More precisely we may state:

Determine if there exist a positive feedback gain γ, and admissible initial conditions $\boldsymbol{q}_0, \Delta\boldsymbol{q}_0$, such that

$$\dot{\boldsymbol{q}}_k^{\text{ref}} = -\gamma \mathbf{J}^{\dagger}(\boldsymbol{q}_k)\boldsymbol{e}(\boldsymbol{q}_k) \tag{3}$$

in closed loop with (1) implies that

$$\lim_{k\to\infty} \|\boldsymbol{e}_k\| = 0. \tag{4}$$

A. Assumptions

In this section we state the assumptions that the stability of $\boldsymbol{e} = 0$ is subject to. These assumptions are the same as considered in [15], and are necessary for a well-posed problem in terms of existence of solutions to (1),(3).

1) $\exists\, \delta \in \mathbb{R}^+ : \|\mathbf{J}(\boldsymbol{q})\| < \delta \quad \forall \boldsymbol{q} \in \mathcal{Q}$
2) $\exists\, \beta \in \mathbb{R}^+ : \underline{\sigma}(\mathbf{J}\mathbf{J}^T) \geq \beta \quad \forall \boldsymbol{q} \in \mathcal{Q}$
3) $\exists\, \zeta \in \mathbb{R}^+ : \|\frac{\partial^2 e_i(\boldsymbol{q})}{\partial \boldsymbol{q}^2}\| \leq \zeta \quad \forall \boldsymbol{q} \in \mathcal{Q}, i \in [1, m]$

Here, as the matrix norm, the spectral norm, i.e., the largest singular value, is used, and $\underline{\sigma}(\mathbf{X})$ denotes the smallest singular value of a matrix $\mathbf{X}$. Assumptions 1) and 3) impose smoothness constraints on the task description, as they assume that the norms of both the Jacobian and the Hessian of $\boldsymbol{e}$ are bounded on $\mathcal{Q}$. These smoothness assumptions hold for example for the direct kinematics of revolute-link manipulators. Assumption 2) specifies that the Jacobian has full rank, and is some *distance* away from a singularity.

B. Preliminaries

The error dynamics will be derived using Taylors theorem with explicit 2nd order Lagrange remainders. We shortly recall the Lagrange remainder result, which is similar to our approach, used in [15] to determine the linearized error-dynamics. From the Taylor expansion of $\boldsymbol{e}(\boldsymbol{q})$ we have

$$\boldsymbol{e}(\boldsymbol{q}+\boldsymbol{\epsilon}) = \boldsymbol{e}(\boldsymbol{q}) + \mathbf{J}(\boldsymbol{q})\boldsymbol{\epsilon} + \boldsymbol{r}(\boldsymbol{q}, \boldsymbol{\epsilon}, \boldsymbol{\zeta}) \tag{5}$$

where the Lagrange remainder $\boldsymbol{r}$ is given by

$$\boldsymbol{r}_i(\boldsymbol{q}, \boldsymbol{\epsilon}, \boldsymbol{\zeta}) = \frac{1}{2}\begin{bmatrix} \boldsymbol{\epsilon}^T \left.\frac{\partial^2 e_1(\boldsymbol{q})}{\partial \boldsymbol{q}^2}\right|_{\boldsymbol{q}+\zeta_1\boldsymbol{\epsilon}} \boldsymbol{\epsilon} \\ \vdots \\ \boldsymbol{\epsilon}^T \left.\frac{\partial^2 e_m(\boldsymbol{q})}{\partial \boldsymbol{q}^2}\right|_{\boldsymbol{q}+\zeta_m\boldsymbol{\epsilon}} \boldsymbol{\epsilon} \end{bmatrix}, \tag{6}$$

for some $\boldsymbol{\zeta} \in \mathbb{R}^m$ where all the elements of $\boldsymbol{\zeta}$ are between 0 and 1, i.e. $\zeta_i \in [\,0\,,\,1\,]$. Note that Assumption 3) implies that $\boldsymbol{r}$ in (5) is quadratically bounded by a norm of $\boldsymbol{\epsilon}$.

The discrete-time variant of Lyapunov's 2nd method for determining the stability of fixed points [18], is also needed for the stability result.

IV. Error dynamics construction

In this section a linearization of the task-error dynamics is constructed. The notation $\mathbf{J}(\boldsymbol{q}_k) = \mathbf{J}_k$ is used for brevity to denote time dependency. The following state error is considered

$$\boldsymbol{z}_k = \begin{bmatrix} \boldsymbol{e}_k \\ \Delta\boldsymbol{q}_k \end{bmatrix}. \tag{7}$$

The joint increments $\Delta\boldsymbol{q}$ are kept in the state to allow us to analyze the stability of the zero dynamics in addition to the error dynamics. This is needed here as $\boldsymbol{e}_k = \mathbf{0}$ or $\Delta\boldsymbol{e}_k = \mathbf{0}$ does not imply that $\Delta\boldsymbol{q}_{k+1} = 0$ for redundant systems. This fact may be seen from inserting $\boldsymbol{e}_k = \mathbf{0}$ in (1),(3). The task velocity $\Delta\boldsymbol{e}_k$ is not included in the state since the feedback law (3) introduces an unmatched task error term which cannot be represented by a task velocity alone.

The proof presented in the next section is a linearization type proof. The goal of this section is hence to derive the dynamics for the state (7) such that the main stabilizing effects of the system appears linearly in the error dynamics, and disturbances/unwanted-effects appears nonlinearly. We will in our analysis group these nonlinear terms denoting them collectively as $\boldsymbol{r}$ for brevity.

The Taylor series of vector-valued functions is the main tool used in the linearization procedure, and the Taylor expansion of the task function may be written as

$$\boldsymbol{e}_{k+1} = \boldsymbol{e}(\boldsymbol{q}_k + \Delta\boldsymbol{q}_{k+1}) = \boldsymbol{e}_k + \mathbf{J}_k\Delta\boldsymbol{q}_{k+1} + \boldsymbol{r}_k. \tag{8}$$

In view of Assumption 3) and standard norm properties, the reminder $\boldsymbol{r}_k$ is bounded as

$$\|\boldsymbol{r}\| \leq \nu\left(\|\mathbf{A}\Delta\boldsymbol{q}_k\| + \gamma T\|\mathbf{A}-\mathbf{I}\|\|\mathbf{J}_k^{\dagger}\|\|\boldsymbol{e}_k\|\right)^2.$$

Using assumptions 1) and 2), [15], the Jacobian pseudo-inverse can be bounded as

$$\|\mathbf{J}^{\dagger}(\boldsymbol{q}_k)\| \leq \frac{\delta}{\beta} = \eta \quad \forall \boldsymbol{q} \in \mathcal{Q}, \tag{9}$$

hence

$$\|\boldsymbol{r}\| \leq \nu_1^2\|\Delta\boldsymbol{q}_k\|^2 + \nu_2^2\|\boldsymbol{e}_k\|^2 + 2\nu_1\nu_2\|\Delta\boldsymbol{q}_k\|\|\boldsymbol{e}_k\| \leq \bar{\nu}\|\boldsymbol{z}_k\|^2,$$

where the positive constants ν_{0-2} and $\bar{\nu}$ are suitably defined. Inserting the dynamics of $\Delta\boldsymbol{q}_k$, (1), and the controller (3) for the 1th order term in the Taylor series gives

$$\mathbf{J}_k\Delta\boldsymbol{q}_{k+1} = \mathbf{J}_k(\mathbf{A}\Delta\boldsymbol{q}_k + \gamma T(\mathbf{A}-\mathbf{I})\mathbf{J}_k^{\dagger}\boldsymbol{e}_k). \tag{10}$$

The state space form of the linearized error dynamics is readily given by (1),(8)

$$\boldsymbol{z}_{k+1} = \underbrace{\begin{bmatrix} \mathbf{I} + \gamma T\mathbf{J}_k(\mathbf{A}-\mathbf{I})\mathbf{J}_k^{\dagger} & \mathbf{J}_k\mathbf{A} \\ \gamma T(\mathbf{A}-\mathbf{I})\mathbf{J}_k^{\dagger} & \mathbf{A} \end{bmatrix}}_{\mathcal{A}_{\mathbf{k}}}\boldsymbol{z}_k + \boldsymbol{r}_k \tag{11}$$

where $\boldsymbol{r}_k$ is quadratic in $\boldsymbol{z}_k$.

V. Stability analysis

In this section the stability properties of the error dynamics derived in the previous section is determined. We will use Lyapunov's 2nd method for discrete-time systems [18], with a quadratic Lyapunov function candidate[1]. The reason behind using Lyapunov's 2nd method, as opposed to more specialized theorems regarding systems with parameter-varying transition matrices, e.g. [19], is that we have a better understanding of the time-variation in the transition matrix, which depends upon $\boldsymbol{q}_k$, than what is typical for a more general

[1] An application originally considered by Hurt in [18] was the stability of the Newton-Raphson method, which is a special case of our system assuming no dynamics in the inner loop and a non-redundant task description.

formulation. This information, which is different from a purely time-varying system, is what allows us to quantify the magnitude of the changes to the transition matrix with respect to the state, and is paramount to completing the proof.

Determining the properties of the configuration dependent transition matrix $\mathcal{A}(\boldsymbol{q}_{\mathbf{k}})$ is the main hurdle in analyzing the stability properties of (11). It is not possible to calculate the eigenvalues of $\mathcal{A}(\boldsymbol{q}_{\mathbf{k}})$ directly since $\mathbf{J}_k$ is a time varying arbitrary matrix, barring the restrictions imposed by Assumptions 1)-3). However, it is possible to estimate the magnitude of the eigenvalues without resorting to direct calculation. The main result in the stability analysis is summarized in the following proposition where $a_{\min}$ denotes the smallest diagonal element of $\mathbf{A}$:

Proposition 1: *If the input gain γ is chosen such that*

$$\gamma < \frac{(1+a_{\min})}{(1-a_{\min})}\frac{2}{T}, \tag{12}$$

and Assumptions 1)-3) hold, then the eigenvalues of $\mathcal{A}(\boldsymbol{q}_{\mathbf{k}})$ are located within the unit circle for all $\boldsymbol{q}_k$. Proof: See Appendix 1.

Proposition 2: *Let $\mathbf{P}_k = \mathbf{P}(\boldsymbol{q}_k)$ be the unique solution to the discrete time Lyapunov equation at the time k*

$$\mathcal{A}_k^T\mathbf{P}_k\mathcal{A}_k - \mathbf{P}_k = -\boldsymbol{I}. \tag{13}$$

If Assumptions 1)-3) hold, and $\mathcal{A}_k$ given by (11) *is a Schur matrix for all k, then the following bound holds for some positive constants ν_1, ν_2*

$$\|\Delta\mathbf{P}_{k+1}\| = \|\mathbf{P}_{k+1} - \mathbf{P}_k\| \le \nu_1\|\boldsymbol{z}_k\| + \nu_2\|\boldsymbol{z}_k\|^2, \tag{14}$$

for either the matrix 2-norm or Frobenius norm. Proof: See Appendix 2.

A. Lyapunov analysis

In this section the 2nd method due to Lyapunov is used to show local asymptotic stability of $\boldsymbol{z} = \mathbf{0}$ for the system (11). For an exposition of Lyapunov theory for discrete time systems see [18]. We will from now on treat the configuration dependency as a time varying exogenous signal. Consider the time varying quadratic Lyapunov function candidate

$$V(k, \boldsymbol{z}_k) = \boldsymbol{z}_k^T\mathbf{P}_k\boldsymbol{z}_k \tag{15}$$

where $\mathbf{P}_k$ is the solution to the discrete time Lyapunov equation

$$\mathcal{A}_k^T\mathbf{P}_k\mathcal{A}_k - \mathbf{P}_k = -\boldsymbol{I}. \tag{16}$$

Under the assumption of Proposition 1, the eigenvalues of $\mathcal{A}_k$ are located wholly within the unit circle, which ensures that $\mathbf{P}_k$ exists and is well-defined [20]. Uniform lower and upper bounds for the Lyapunov function are given as

$$\lambda_m\{\mathbf{P}\}\|\boldsymbol{z}_k\|^2 \le V(k, \boldsymbol{z}_k) \le \lambda_M\{\mathbf{P}\}\|\boldsymbol{z}_k\|^2 \tag{17}$$

Where $\lambda_m\{\mathbf{P}\}, \lambda_M\{\mathbf{P}\}$ denotes the lower and upper bounds for the eigenvalue of $\mathbf{P}(\boldsymbol{q}_k)$ uniformly in $\boldsymbol{q}_k$. For a derivation of the smallest and largest eigenvalues of $\mathbf{P}_k$ explicitly, see [20].

The Lyapunov difference $\Delta V_{k+1} = V_{k+1} - V_k$ is calculated as

$$\Delta V_{k+1} = (\mathcal{A}_k\boldsymbol{z}_k + \boldsymbol{r}_k)^T\mathbf{P}_{k+1}(\mathcal{A}_k\boldsymbol{z}_k + \boldsymbol{r}_k) - \boldsymbol{z}_k^T\mathbf{P}_k\boldsymbol{z}_k. \tag{18}$$

Expanding (18) and collecting the superquadratic terms in r gives

$$\Delta V_{k+1} \le \boldsymbol{z}_k^T\left[\mathcal{A}_k^T(\mathbf{P}_k + \Delta\mathbf{P}_{k+1})\mathcal{A}_k - \mathbf{P}_k\right]\boldsymbol{z}_k + r_k. \tag{19}$$

Imposing the bound from Proposition 2, and lumping the superquadratic terms in r

$$\Delta V_{k+1} \le \boldsymbol{z}_k^T\underbrace{\left[\mathcal{A}_k^T\mathbf{P}_k\mathcal{A}_k - \mathbf{P}_k\right]}_{-\mathbf{I}}\boldsymbol{z}_k + r_k. \tag{20}$$

which we see is locally negative definite using the definition of $\mathbf{P}_k$ (16)

$$\Delta V_{k+1} \le -\|\boldsymbol{z}_k\|^2 + r_k \tag{21}$$

because r_k depends upon cubic powers of $\|z_k\|$ and higher. Together with the upper and lower boundedness of the Lyapunov function in terms of the state, we can using Lyapunov's 2nd method [18] summarize our result as follows.

Theorem 1: *If the feedback gain γ is chosen small enough to fulfill Proposition 1, and Assumptions 1)-3) hold, then there exists a small enough initial conditions $\|\Delta\boldsymbol{q}_0\|, \|\boldsymbol{e}_0\|$ such that $\boldsymbol{z}_k = 0$ is an asymptotically stable equilibrium point of the system* (1),(3)*, i.e.*

$$\lim_{k\to\infty}\|\boldsymbol{e}_k\| = 0, \quad \lim_{k\to\infty}\|\Delta\boldsymbol{q}_k\| = 0.$$

VI. Qualitative considerations

Note that if $a_i = 0$, i.e. the homogeneous perfect control assumption which is common in the literature, then the upper gain margin is $\gamma < \frac{2}{T}$, which is identical to the one derived by [15]. The previous result may hence be seen as a special case of the more general result derived here. We also observe that a slower velocity controller implies that a higher gain is possible. An oscillatory controller with $a_{\min} = -1 + \epsilon$ for $\epsilon \ll 1$ is the worst case, in which we have an upper bound on the order of $\frac{\epsilon}{T}$. This means that if a platoon of robots is controlled centrally using the RMRC, then the gain margin is limited by the robot with the worst inner-loop response. It is also observed that for all inner-loop dynamics, a higher sampling frequency imply that higher input gains are possible while maintaining stability.

VII. Conclusion and Further work

It was shown in this paper that the RMRC (3) used for outer-loop kinematic control with a 1th order linearly stable inner loop (1), results in an asymptotically stable task error and zero-dynamics. The result is applicable to both minimum and non-minimum phase heterogeneous discrete-time dynamics in the inner loop. A tight upper bound for the outer-loop feedback gain was derived. Furthermore, it was seen that slower low-level joint control implies that a higher outer-loop feedback gain is possible while maintaining stability.

The results extend the knowledge of the stability properties of applications such as, redundancy control, centralized coordinated robotic systems with non-identical agents, visual servoing, and motion control of industrial manipulators with different servo motor responses. A more realistic feedback bound for these systems is derived, which simplifies gain tuning. For a multi agent system for instance, it was seen that the "worst" behaved agent limits the upper bound on the centralized feedback gain.

The future efforts to generalize the results will mainly consist adding input/output delays for a more general inner loop.

VIII. ACKNOWLEDGMENTS

This work is part of the research project Next Generation Robotics for Norwegian Industry. The project partners are The Research Council of Norway, SINTEF, NTNU, Statoil, Hydro, Tronrud Engineering, SbSeating, Glen Dimplex Nordic and RobotNorge.

APPENDIX
PROOF OF PROPOSITION 1

To show that Proposition 1 is true, note that the matrix $\mathcal{A}(\boldsymbol{q_k})$ has the following factorization

$$\mathcal{A}(\boldsymbol{q_k}) = \mathbf{S_k B S_k^T}(\mathbf{S_k S_k^T})^{-1} \tag{22}$$

$$\mathbf{S}_k = \begin{bmatrix} \mathbf{J}_k & \mathbf{0}_{m\times n} \\ \mathbf{0}_{n\times n} & \mathbf{I}_{n\times n} \end{bmatrix} \tag{23}$$

$$\mathbf{B} = \begin{bmatrix} \mathbf{I} + \gamma T(\mathbf{A} - \mathbf{I}) & \mathbf{A} \\ \gamma T(\mathbf{A} - \mathbf{I}) & \mathbf{A} \end{bmatrix} \tag{24}$$

Here $\mathbf{S}_k \in \mathbb{R}^{n+m\times 2n}$, and $\mathbf{B} \in \mathbb{R}^{2n\times 2n}$. This factorization is possible since $\mathbf{J}_k\mathbf{J}_k^\dagger = \mathbf{I}$ as $\mathbf{J}_k$ has full rank by using Assumption 2). Now consider an eigenvalue/eigenvector pair $\boldsymbol{v} \in \mathbb{C}^{n+m}$,$\lambda \in \mathbb{C}$, where $\boldsymbol{v} \neq \mathbf{0}$

$$\mathbf{S}_k\mathbf{B}\mathbf{S}_k^T(\mathbf{S}_k\mathbf{S}_k^T)^{-1}\boldsymbol{v} = \lambda\boldsymbol{v}. \tag{25}$$

The configuration dependency is first moved to the first m equations of (25) using the change of variables $\boldsymbol{u} = (\mathbf{S}_k\mathbf{S}_k^T)^{-1}\boldsymbol{v}$ such that

$$\mathbf{S}_k\mathbf{B}\underbrace{\mathbf{S}_k^T\boldsymbol{u}}_{\boldsymbol{z}} - \lambda\mathbf{S}_k\underbrace{\mathbf{S}_k^T\boldsymbol{u}}_{\boldsymbol{z}} = \mathbf{0} \;\Rightarrow\; \mathbf{S}_k(\mathbf{B}\boldsymbol{z} - \lambda\boldsymbol{z}) = 0. \tag{26}$$

It is seen that we can now define $\boldsymbol{z} = \mathbf{S}_k^T\boldsymbol{u}$ even though this transformation is not invertible.Furthermore, note that $\boldsymbol{z}$ is in the range of $\mathbf{S}_k^T$ such that $\mathbf{S}_k^\dagger\mathbf{S}_k\boldsymbol{z} = \boldsymbol{z}$. The last n equations of (26) which are now configuration free are given by

$$\gamma T(\mathbf{A} - \mathbf{I})\boldsymbol{z}_1 + \mathbf{A}\boldsymbol{z}_2 = \lambda\boldsymbol{z}_2 \tag{27}$$

where $\boldsymbol{z}^T = [\boldsymbol{z}_1^T, \boldsymbol{z}_2^T]^T$. Since the elements of $\mathbf{A}_{i,i} \in (-1, 1)$ then $(\mathbf{A} - \mathbf{I})$ is invertible, and we note that both $\boldsymbol{z}_1^T, \boldsymbol{z}_2^T$ are nonzero and that (27) has a unique solution for $\boldsymbol{z}_2$ in terms of $\boldsymbol{z}_1$ and λ. Inserting this solution into the top m equations of (26) gives

$$\mathbf{J}_k[\mathbf{I} + \gamma T(\mathbf{A} - \mathbf{I}) - T\gamma\mathbf{A}(\mathbf{A} - \lambda\mathbf{I})^{-1}(\mathbf{A} - \mathbf{I})) - \lambda\mathbf{I}]\boldsymbol{z}_1 = \mathbf{0}$$

This equation is rendered configuration free by a pre-multiplication of $\boldsymbol{z}_1^H\mathbf{J}_k^\dagger$ using the fact that $\boldsymbol{z}_1$ is in the range of $\mathbf{J}_k^T$, resulting in the scalar equation

$$\boldsymbol{z}_1^H[\mathbf{I} + \gamma T(\mathbf{A} - \mathbf{I}) - T\gamma\mathbf{A}(\mathbf{A} - \lambda\mathbf{I})^{-1}(\mathbf{A} - \mathbf{I})) - \lambda\mathbf{I}]\boldsymbol{z}_1 = 0.$$

Here $\boldsymbol{z}_1^H = (\boldsymbol{z}_1^T)^*$ denotes the hermitian transposed where $(x + jy)^* = (x - jy)$ is the complex conjugate and j is the purely imaginary number. One further change of variables given by $\boldsymbol{\zeta} = (\mathbf{A} - \lambda\mathbf{I})\boldsymbol{z}_1$ is introduced to remove the inverse matrix $(\mathbf{A} - \lambda\mathbf{I})^{-1}$. The complex vector $\boldsymbol{\zeta}$ is normalized such that $\boldsymbol{\zeta}^H\boldsymbol{\zeta} = 1$. This transformation is not well-defined for $\lambda = a_i$. In this case the proof is done however as $|\lambda| = |a_i| < 1$. For the cases where $\lambda \neq a_i$ we apply the transformation yielding

$$\boldsymbol{\zeta}^H(\mathbf{A} - \lambda^*\mathbf{I})(\lambda^2\mathbf{I} + (T\gamma(\mathbf{I} - \mathbf{A}) - \mathbf{A} - \mathbf{I})\lambda + \mathbf{A})\boldsymbol{\zeta} = 0.$$

At this point we are ready to impose some restrictions on the magnitude of the eigenvalue λ. The real and complex cases for $\lambda = x + jy$ will be handled seperately. The real and imaginary part of $\boldsymbol{\zeta}^H[...]\boldsymbol{\zeta}$ is calculated as

$$\boldsymbol{\zeta}^H[\mathbf{D}x + (T\gamma(\mathbf{A} - \mathbf{I}) + \mathbf{I} - x\mathbf{I})|\lambda|^2 - 2\mathbf{A}x + \mathbf{A}^2]\boldsymbol{\zeta} = 0 \tag{28}$$

$$y\boldsymbol{\zeta}^H(\mathbf{D} - |\lambda|^2\mathbf{I})\boldsymbol{\zeta} = 0 \tag{29}$$

where

$$\mathbf{D} = \mathbf{A}[-\mathbf{A}(T\gamma + 1) + 2x\mathbf{I} + T\gamma\mathbf{I}] \tag{30}$$

1) The complex case: Let $y \neq 0$. From (29) it is seen that $\boldsymbol{\zeta}^H(\mathbf{D} - |\lambda|^2\mathbf{I})\boldsymbol{\zeta} = 0$. We may solve (29) easily for x as it is now a linear equation in x, and insert the solution into (28) giving

$$-T\gamma\boldsymbol{\zeta}^H(\mathbf{A} - \mathbf{I}|\lambda|^2)(\mathbf{A} - \mathbf{I})\boldsymbol{\zeta} = 0, \tag{31}$$

which we can solve as

$$|\lambda|^2 = \boldsymbol{\zeta}_2^H\mathbf{A}\boldsymbol{\zeta}_2 = \tilde{a} < 1, \quad \|\boldsymbol{\zeta}_2\| = 1 \tag{32}$$

where $\boldsymbol{\zeta}_2 = (\mathbf{I} - \mathbf{A})^{\frac{1}{2}}\boldsymbol{\zeta}$. Since $\|\boldsymbol{\zeta}_2\| = 1$ and $\mathbf{A}$ is a real diagonal matrix, then $\tilde{a}$ is a real number in the range $[a_{\min}, a_{\max}]$. In summary, if an eigenvalue of $\mathcal{A}_k$ is imaginary, then the eigenvalue is located within the unit circle for all feedback gains γ. Moreover, if a_i are all negative, then all the eigenvalues are real.

2) The real case: Let $y = 0$. In this case (28) is a 3d order polynomial in x with only real solutions. We will show that under the conditions of Proposition 1, λ cannot be equal to 1 or -1. Since the eigenvalues varies continuously with the elements of $\mathcal{A}_k$, then $\lambda \neq \pm 1$ implies that number of real eigenvalues outside the unit circle is constant for all $\boldsymbol{q}_k$. Inserting $x = 1, y = 0$ into (28) gives

$$-T\gamma\boldsymbol{\zeta}^H(\mathbf{A} - \mathbf{I})^2\boldsymbol{\zeta} = 0, \tag{33}$$

which can not be equal to zero since $(\mathbf{A} - \mathbf{I})^2$ is a diagonal matrix with strictly positive elements. Inserting $x = -1, y = 0$ into (28) gives

$$\boldsymbol{\zeta}^H(\mathbf{A} + \mathbf{I})\underbrace{(2(\mathbf{A} + \mathbf{I}) + T\gamma(\mathbf{A} - \mathbf{I}))}_{\mathbf{G}}\boldsymbol{\zeta} = 0 \tag{34}$$

For equation (34) to hold, then all the elements of $\mathbf{G}$ cannot have the same sign since $(\mathbf{A} + \mathbf{I})$ is positive definite. The elements of $\mathbf{G}$ are all positive if

$$\gamma < \frac{(1+a_{\min})}{(1-a_{\min})}\frac{2}{T} \tag{35}$$

which is seen by solving $G_i > 0$ for γ. To verify that the constant number of real roots outside the unit circle is zero, we may for instance take $\mathbf{J} = \mathbf{I}$ and apply Jury's test resulting in (35), or test a single case numerically. This completes the proof of Proposition 1.

APPENDIX
PROOF OF PROPOSITION 2

The derived bound (14) relies on a result from [20], which quantifies how the solution to the discrete time Lyapunov equation varies with perturbations to the transition matrix. The following bound which holds for the 2-norm and Frobenius matrix norm, is derived in [20] for $\Delta\mathbf{P}_{k+1}$

$$\|\Delta\mathbf{P}_{k+1}\| \le \|\mathbf{P}_{k+1}\|\|\mathbf{P}_k\|\|\Delta\mathcal{A}_{k+1}\|(2\|\mathcal{A}_k\| + \|\Delta\mathcal{A}_{k+1}\|). \tag{36}$$

Furthermore there exist a positive constants ρ_k such that

$$\|\mathbf{P}_k\| \le \rho_k \tag{37}$$

We define the upper bound uniformly in $\boldsymbol{q}$ as

$$\|\mathbf{P}_k\| \le \alpha = \sup_{\boldsymbol{q}\in\mathcal{Q}} \rho(\boldsymbol{q}) \tag{38}$$

It is possible to bound the change of the linearized transition matrix $\Delta\mathcal{A}_{k+1}$ by the state $\boldsymbol{z}_k$. This is due to the boundedness of the partial derivatives of the task Jacobian by Assumption 3), we can construct the following Taylor expansion for $\mathbf{J}$

$$\mathbf{J}(\boldsymbol{q}_k + \Delta\boldsymbol{q}_{k+1}) = \mathbf{J}_k + \mathbf{H}(\Delta\boldsymbol{q}_{k+1}, \boldsymbol{\zeta})$$

For some constants ζ_i in the range $(0,1)$ which are possibly different from those from (6). The elements of $\mathbf{H}$ may be calculated using the Hessian of the task function $\boldsymbol{e}$ as in (6). It is seen that the task Jacobian difference is bounded as $\Delta\mathbf{J}_{k+1} = \mathbf{J}_{k+1} - \mathbf{J}_k = \mathbf{H}(\Delta\boldsymbol{q}_{k+1}, \boldsymbol{\zeta})$ such that

$$\|\Delta\mathbf{J}_{k+1}\| = \|\mathbf{H}(\Delta\boldsymbol{q}_{k+1}, \boldsymbol{\zeta})\| \le \alpha_2\|\Delta\boldsymbol{q}_{k+1}\| \le \alpha_2^{'}\|\boldsymbol{z}_k\| \tag{39}$$

for some positive constants $\alpha_2, \alpha_2^{'}$. The task Jacobian pseudoinverse is bounded similarly using Taylor's theorem and noting that the partial derivatives of $\mathbf{J}_k^{\dagger}$ with respect to $\boldsymbol{q}$ are given by

$$\frac{\partial}{\partial q_i}\mathbf{J}^{\dagger} = (\partial\mathbf{J})^T(\mathbf{J}\mathbf{J}^T)^{-1} - \mathbf{J}^{\dagger}[(\partial\mathbf{J})\mathbf{J}^T + \mathbf{J}(\partial\mathbf{J})^T](\mathbf{J}\mathbf{J}^T)^{-1},$$

with

$$\partial\mathbf{J} = \frac{\partial}{\partial q_i}\mathbf{J}_k, \quad \|\partial\mathbf{J}\| \le \nu^{'}\|\Delta\boldsymbol{q}_{k+1}\|. \tag{40}$$

The obtained bound $\|\partial\mathbf{J}_k^{\dagger}\| \le \eta\|\boldsymbol{z}_k\|$ is due to Assumption 1) which bounds the Jacobian, $(\mathbf{J}\mathbf{J}^T)^{-1}$ is bounded using Assumption 2) and Assumption 3) is used to obtain (40). As the partial derivatives of the elements of the task Jacobian and its pseudoinverse are bounded, we have that the partial derivatives of the elements of the transition matrix $\mathcal{A}_k$, which are linear combinations of these, also are bounded. Expressing the bounds for the task Jacobian difference (39), and for $\Delta\mathbf{J}_k^{\dagger}$ in terms of $\mathcal{A}_k$ gives

$$\|\Delta\mathcal{A}_{k+1}\| \le \nu\|\boldsymbol{z}_k\|, \quad \nu > 0. \tag{41}$$

The proof is completed by inserting (38),(39),(41) into (36) giving

$$\|\Delta\mathbf{P}_{k+1}\| \le \nu_1\|\boldsymbol{z}_k\| + \nu_2\|\boldsymbol{z}_k\|^2. \tag{42}$$

REFERENCES

[1] T. Fossen, *Handbook of Marine Craft Hydrodynamics and Motion Control*. John Wiley & Sons, 2011.

[2] B. Siciliano and O. Khatib, *Springer handbook of robotics*, 2008.

[3] K. Nilsson, "Industrial robot programming," Ph.D. dissertation, Lund Institute of Technology, Department of Automatic Control,Department of Automatic Control, Sweden, 1996.

[4] M. Aicardi, A. Caiti, G. Cannata, and G. Casalino, "Stability and robustness analysis of a two layered hierarchical architecture for the closed loop control of robots in the operational space," in *Robotics and Automation, 1995. Proceedings., 1995 IEEE International Conference on*, vol. 3, may 1995, pp. 2771 –2778 vol.3.

[5] D. Whitney, "Resolved motion rate control of manipulators and human prostheses," *IEEE Transactions on Man-Machine Systems*, vol. 10, no. 2, pp. 47 –53, june 1969.

[6] A. Balestrino, G. De Maria, and L. Sciavicco, "Robust control of robotic manipulators," in *9th IFAC World Congress, 1984. Proceedings*, vol. VI, july. 1984, pp. 80 – 85.

[7] S. Hutchinson, G. Hager, and P. Corke, "A tutorial on visual servo control," *IEEE Transactions on Robotics and Automation.*, vol. 12, no. 5, pp. 651 –670, oct 1996.

[8] B. Siciliano, "Kinematic control of redundant robot manipulators: A tutorial," *Journal of Intelligent and Robotic Systems*, vol. 3, no. 3, pp. 201–212, 1990.

[9] S. Ahmad and S. Luo, "Coordinated motion control of multiple robotic devices for welding and redundancy coordination through constrained optimization in cartesian space," *IEEE Transactions on Robotics and Automation*, vol. 5, no. 4, pp. 409 –417, aug 1989.

[10] J. Moreno and R. Kelly, "Hierarchical velocity field control for robot manipulators," in *Robotics and Automation, 2003. Proceedings. ICRA '03. IEEE International Conference on*, vol. 3, sept. 2003, pp. 4374 – 4379 vol.3.

[11] O. Khatib, "A unified approach for motion and force control of robot manipulators: The operational space formulation," *IEEE Journal of Robotics and Automation*, vol. 3, no. 1, pp. 43–53, 1987.

[12] R. Kelly and J. Moreno, "Manipulator motion control in operational space using joint velocity inner loops," *Automatica*, vol. 41, no. 8, pp. 1423–1432, 2005.

[13] K. Camarillo, R. Campa, V. Santibáñez, and J. Moreno-Valenzuela, "Stability analysis of the operational space control for industrial robots using their own joint velocity pi controllers," *Robotica*, vol. 26, no. 6, p. 729.

[14] J. Nocedal and S. Wright, *Numerical optimization*. Springer verlag, 1999.

[15] P. Falco and C. Natale, "On the stability of closed-loop inverse kinematics algorithms for redundant robots," *IEEE Transactions on Robotics*, no. 99, pp. 1–5, 2011.

[16] B. Bishop, "On the use of redundant manipulator techniques for control of platoons of cooperating robotic vehicles," *IEEE Transactions on Systems, Man and Cybernetics, Part A: Systems and Humans.*, vol. 33, no. 5, pp. 608–615, 2003.

[17] E. Conkur and R. Buckingham, "Clarifying the definition of redundancy as used in robotics," *Robotica*, vol. 15, no. 05, pp. 583–586, 1997.

[18] J. Hurt, "Some stability theorems for ordinary difference equations," *SIAM Journal on Numerical Analysis*, pp. 582–596, 1967.

[19] F. Amato, M. Mattei, and A. Pironti, "A note on quadratic stability of uncertain linear discrete-time systems," *IEEE Transactions on Automatic Control,*, vol. 43, no. 2, pp. 227 –229, feb 1998.

[20] P. Gahinet, A. Laub, C. Kenney, and G. Hewer, "Sensitivity of the stable discrete-time lyapunov equation," *IEEE Transactions on Automatic Control,*, vol. 35, no. 11, pp. 1209 –1217, nov 1990.